Core level ionization dynamics in small molecules studied by x-ray-emission threshold-electron coincidence spectroscopy

Michele Alagia,[1] Robert Richter,[2] Stefano Stranges,[3,4] Marcus Agåker,[5] Magnus Ström,[5] Johan Söderström,[5] Conny Såthe,[5] Raimund Feifel,[6] Stacey Sorensen,[7] Alberto De Fanis,[8] Kiyoshi Ueda,[9] Reinhold Fink,[4] and Jan-Erik Rubensson[4]

[1]*CNR-ISMN, Sezione Roma1, Piazale A. Moro 5, I-00185 Rome, Italy*
[2]*Sincrotrone Trieste, Area Science Park, Basovizza, I-34012 Trieste, Italy*
[3]*Dipartimento di Chimica, Università La Sapienza, I-00185 Roma*
[4]*TASC-INFM Laboratory, Area Science Park, Basovizza 34012 Trieste, Italy*
[5]*Physics Department, Box 530, S-751 21 Uppsala, Sweden*
[6]*Physical and Theoretical Chemistry Laboratory, Oxford University, South Parks Road, Oxford OX1 3QZ, United Kingdom*
[7]*Department of Synchrotron Radiation Research, University of Lund, S-221 00 Lund, Sweden*
[8]*Nanotechnology Division, JASRI/SPring-8, 1-1-1 Kouto Mikazuki-cho, Sayo-gun Hyogo 679-5198, Japan*
[9]*Institute of Multidisciplinary Research for Advanced Materials, Tohoku University, Sendai 980-8577, Japan*

X-ray-emission threshold-electron coincidence spectroscopy has been applied to N_2, O_2, and N_2O. The main features of the spectra can be interpreted as conventional core level threshold electron spectra, free from postcollision interaction effects. The relative cross sections for adiabatic ionization of close-lying core hole states and vibrational substates are presented. The results are compared to theoretical predictions and state-of-the-art photoelectron spectra and are discussed in terms of direct threshold ionization and core vacancy rearrangement processes.

The excitation-energy dependence of core level ionization cross sections has been investigated for several systems (see, e.g., [1,2]). In the immediate threshold vicinity, ionization dynamics is manifested in the postcollision interaction (PCI) between the slow photoelectron and the Auger electron emitted in the core hole decay. The features in x-ray-photoemission spectra (XPS) are energetically displaced and broadened by the PCI effect [3]. This complicates the evaluation of the data, especially in the adiabatic limit, which is probed by threshold photoelectron (TPE) spectroscopy [4].

To fully exploit TPE spectroscopy in the study of core level threshold ionization cross sections the PCI effect must be eliminated. Some years ago it was shown that this can be done by measuring the electrons in coincidence with soft x-ray photons [5]. Here we have substantially improved this x-ray-emission threshold-electron coincidence (XETECO) technique. The energy resolution is now better than in state-of-the-art photoelectron spectra, which we have recorded for comparison, and the data quality allows for peak shape analysis.

We present the XETECO spectra of N_2, O_2, and N_2O. In these molecules the relative intensities of close-lying core-ionized states, as well as of clearly resolved vibrational excitations, are presented. The relative intensities are discussed in terms of XPS excited close to threshold and theoretical predictions of direct threshold ionization cross sections. We also consider coupling between the ionization continuum and degenerate discrete autoionizing states, which frequently plays an important role in low-energy TPE spectroscopy [6]. At core thresholds, the autoionization channel involves a core vacancy rearrangement (CVR), competing with the core hole decay. The three cases studied here represent three entirely different CVR mechanisms: parity change in N_2, spin

flip in O_2, and interatomic core vacancy transfer in N_2O.

The XETECO spectra were measured at the gas-phase beamline [7] at ELETTRA, using an electron analyzer based on the penetration-field technique [8]. The energy resolution of this instrument was around 10 meV for the N_2 and N_2O experiment and 30 meV for the O_2 experiment, and hence the total instrumental energy resolution was determined almost entirely by the monochromator. A photon detector was positioned close to the interaction region to cover a large solid angle (approximately 10%). The emitted soft x-ray photons were measured in the direction of polarization of the primary photon beam. For reference, conventional XPS measurements were performed at beamline 27SU at SPring-8 using a high-resolution electron spectrometer SES-2002 (Gammadata-Scienta) [9]. Here, the XPS results are used for reference only, and they will be discussed in detail elsewhere.

The fluorescence yield (FY) spectra (Figs. 1–3) are similar to soft x-ray absorption (SXA) spectra, whereas the TPE spectra are dominated by broad structures with the on-set close to the core level ionization thresholds. The coincidences between these two channels, constituting the XETECO spectra, show sharp peaks with intensity maxima at 0.2–0.3 eV lower energy than the TPE spectra. The relative energy calibration of these three spectra is ensured, because they are recorded in the same energy scan, and the absolute calibration is facilitated by aligning the Rydberg series seen in FY and TPE spectra to SXA literature values. The figures include photoelectron spectra excited well above threshold for comparison.

The XETECO spectrum of N_2 (Fig. 1) shows two prominent peaks at 409.82 and 409.93 eV, which we assign to adiabatic transitions to the ungerade and gerade core-ionized
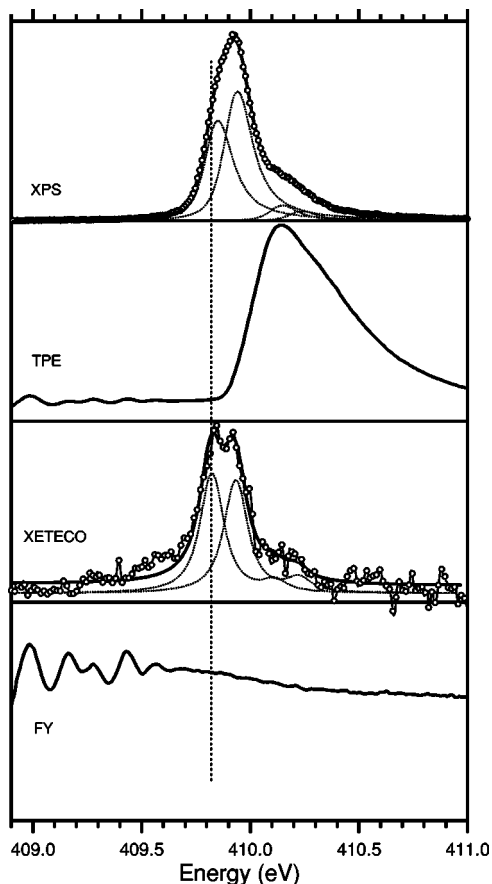
FIG. 1. The ungerade (low-energy) and gerade (high-energy) nitrogen 1 s thresholds of the N_2 molecule. The excitation energy for XPS is 460 eV. At the low-energy side both TPE and FY spectra show features corresponding to Rydberg excitations in the absorption spectrum. The shift between the main peaks in XETECO and TPE spectra is a direct measure of the threshold PCI shift. The estimated instrumental resolution is 40 meV and 70 meV for XETECO and XPS, respectively.

states, respectively. The two states are seen also in XPS using curve fitting procedures [2]. The absolute difference in energy position between XETECO and (independently calibrated) XPS peaks is less than 40 meV, and an ungerade-gerade energy split of 0.1 eV is found with both techniques. In the XPS spectrum excited at 460 eV the ungerade/gerade intensity ratio is 0.8. This deviation from the statistically expected value of unity agrees with earlier experimental results as well as theoretical predictions ([2] and references therein). In XETECO the intensity ratio is 1.1, which is also in line with the earlier results for the ionization cross sections. In addition, both XPS and XETECO spectra show a structure around 410.2 eV, which is due to excitation of the $v=1$ vibration. The fit result gives a $v=1/v=0$ intensity which is higher for the gerade state than for the ungerade in XETECO, whereas the opposite is true in XPS, fully in line with what is expected from an extrapolation of the measured excitation-energy dependence in Ref. [2].

The interpretation of the XETECO spectrum as a PCI-free TPE spectrum is thus corroborated both by the agreement with XPS and by the discrepancy with the noncoincident
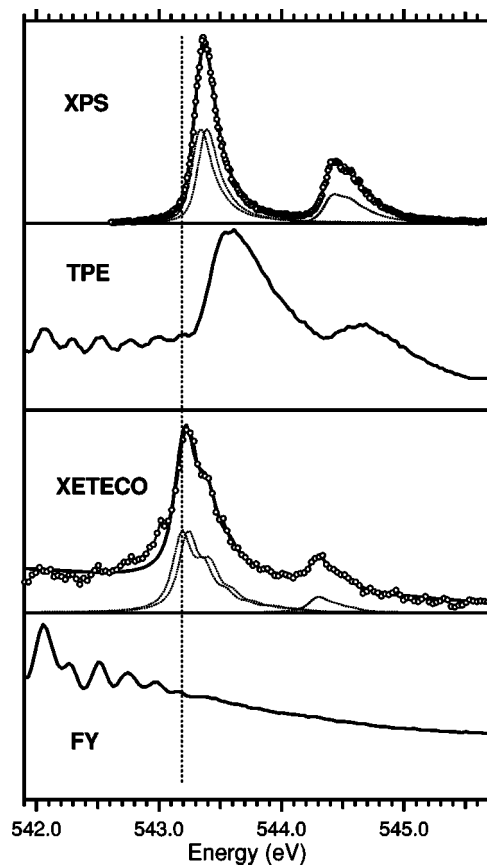

FIG. 2. The quartet (low energy) and doublet (high energy) 1 s thresholds of the O_2 molecule. The excitation energy for XPS is 590 eV. The estimated instrumental broadening is 80 meV, both for XETECO and XPS. The fits are based on theoretical values for the ungerade-gerade split [12], 50 meV and 7 meV, for the quartet and doublet, respectively.

TPE spectrum, which can be accounted for by the influence of PCI on the latter.

The XETECO intensity may, however, be influenced by variations in fluorescence probability. In a two-step approximation, the ratio between the intensities of the energetically lower (ungerade), I_L, and higher (gerade), I_H, states is related to the oscillator strength associated with *direct* threshold ionization cross sections f_L and f_H:

$$\left(\frac{I_L}{I_H}\right)_{Direct} = \frac{f_L \omega_L}{f_H \omega_H}, \tag{1}$$

where $\omega_L = \Gamma_{X,L}/\Gamma_{tot,L}$ and $\omega_H = \Gamma_{X,H}/\Gamma_{tot,H}$ are the probabilities for the specific x-ray decay, associated with photons emitted in the solid angle covered by the photon detector. $\Gamma_{X,L}$ and $\Gamma_{X,H}$ are the corresponding x-ray decay rates, and $\Gamma_{tot,L}$ and $\Gamma_{tot,H}$ are the total core hole decay rates, dominated by the Auger channel. High-energy excited x-ray emission spectra suggest that ω_L/ω_H is slightly smaller than unity [10]. In addition, there is a symmetry-dependent angular anisotropy [10], which makes the XETECO signal sensitive to the symmetry of the continuum at threshold. Although these effects should be included in a rigorous description, they are not large enough to influence the discussion, and we do not
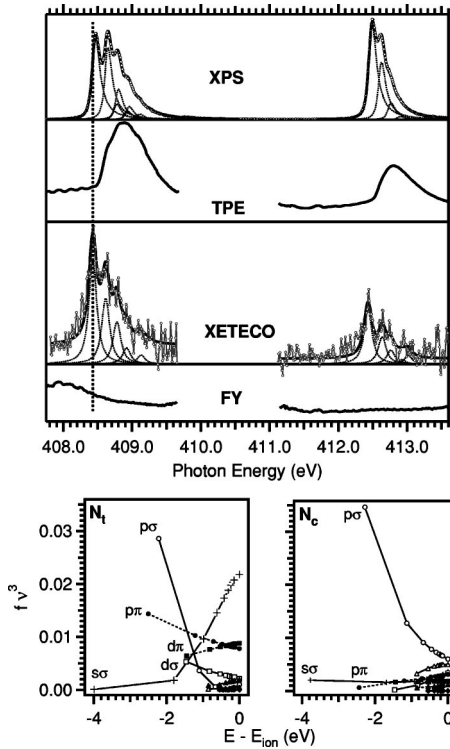
FIG. 3. The terminal (low-energy) and central (high-energy) nitrogen 1 s thresholds of the N_2O molecule. The excitation energy for XPS is 480 eV. The estimated instrumental resolution is 40 meV both for XETECO and XPS. The lowest panel shows the oscillator strengths scaled by the energy density of the corresponding Rydberg series.

attempt any quantitative correction of the present data.

The results obtained for O_2 are shown in Fig. 2. The energy difference between ungerade and gerade core-ionized states of the O_2 molecule is too small [11,12] to be resolved in the present measurement. The 1s threshold is further split due to the exchange interaction between the unpaired core electron and the two electrons in the outermost orbital. The most intense peak in both XETECO and XPS is due to transitions to the quartet coupled states. A curve fit (assuming equal weight of ungerade and gerade components) has the $v=0$ component of the ungerade quartet state at 543.19 eV (XETECO) and 543.34 eV (XPS). The quartet and doublet states are found to be separated by 1.09 eV in the XETECO spectrum, compared to 1.06 eV in XPS. We attribute these small discrepancies to calibration errors.

There are two remarkable differences between the XPS and XETECO spectra: First, vibrational excitations in the quartet state are much more intense in XETECO than in XPS. A fit gives a $v=1/v=0$ intensity ratio of 0.52 in XETECO, whereas this value is very small in XPS. Second, the quartet/doublet total intensity ratio is around 6 in XETECO, while the XPS intensity ratio is found to be around 2.2.

As there are no large differences in fluorescence probability for the spin states in the oxygen ion [13,14] we interpret the principal discrepancies between XETECO and XPS intensities as due to differences in the ionization cross sections at threshold.

Several factors may influence the threshold intensities, e.g., the proximity to the σ^* resonances in O_2, which may preferentially enhance the cross section of the lower level. To our knowledge, there are no data on the intensity ratio in XPS excited close to threshold from which trends can be extrapolated. We find a monotonous *decrease* of the intensity ratio from 2.2 at 590 eV excitation energy to 1.5 (not shown) 10 eV above threshold excitation.

In addition to direct threshold ionization, we consider autoionization of neutral states associated with higher-lying thresholds, which frequently influences the total ionization cross section as well as the vibrational progressions in TPE spectra of underlying states [4,6]. For core levels such processes compete with the core hole decay. In a simple multistep model an indirect CVR channel would modify the intensity ratio:

$$\frac{I_L}{I_H} \approx \frac{\left(f_L + f_H^R \dfrac{\Gamma_{CVR}}{\Gamma_{CVR} + \Gamma_A}\right)\omega_L}{f_H \omega_H}$$

$$= \left(\frac{I_L}{I_H}\right)_{direct}\left(1 + \frac{f_H^R}{f_L}\frac{\Gamma_{CVR}}{\Gamma_{CVR} + \Gamma_A}\right), \qquad (2)$$

where Γ_{CVR} and Γ_A are the CVR rate and the Auger core hole decay rate (the radiative rate is neglected), respectively, and f_H^R is the oscillator strength for resonant excitation of a neutral state associated with the energetically higher threshold. In this case, the considered CVR process is spin-flip autoionization of neutral states with a doublet coupled core to quartet core hole states. Requirements for a significant influence of this process on the XETECO intensity are elucidated by Eq. (2): Γ_{CVR} must be comparable to Γ_A, and/or f_H^R must be comparable to f_L.

As in low-energy TPE spectra, non-Franck-Condon population of vibrational states gives access to parts of the core level potential curve, which are not reached in conventional XPS. The curve fitting procedure gives a quartet vibrational spacing of 179 meV in the XETECO spectrum.

The N_2O molecule (Fig. 3) has two chemically shifted core ionization thresholds associated with the terminal, N_T (408.43 eV in XETECO, 408.44 eV in XPS), and the central, N_C [$E(N_T)+4.01$ eV in XETECO, $E(N_T)+4.02$ eV in XPS], nitrogen atoms. The principal differences between XPS and XETECO spectra are analogous to the O_2 case. First, the vibrational progression in the low-energy peak is significantly different: in XETECO, the relative intensity of the $v=0$ transition is much larger than in high-energy XPS. Second, the N_T/N_C intensity ratio is around 2.5 in XETECO, compared to 1.1 in XPS. Also in this case, $\omega_L/\omega_H \approx 1$ [15], and we interpret the differences as due to changes in the threshold ionization cross section.

We obtained a theoretical value for f_L/f_H by extrapolating calculated oscillator strengths for transitions to highly excited Rydberg states to the ionization energy. The Rydberg states were described in the improved virtual orbitals approximation using Hartree-Fock wave functions for the core-ionized states and a basis set that can represent s, p, d, f, and g Rydberg orbitals up to effective principal quantum num-

bers v of 10 [16]. These Rydberg-state representations and the Hartree-Fock ground state gave rise to oscillator strengths f, which are plotted in the bottom part of Fig. 3 where they are multiplied by the energy density v^3. This factor leads to a normalization per unit energy and thus accounts for the infinite density of Rydberg states in a small range near the ionization threshold, causing the finite XE-TECO signal. This procedure leads to a smooth transition towards (and beyond) the ionization threshold [17]. In Fig. 3 the s-to-g Rydberg series of σ and π symmetries are connected by straight lines and extrapolated as $v \to \infty$. The threshold ionization oscillator strengths are the sums of the extrapolated values and lead to the theoretical value of $f_L/f_H \approx 1.8$. The large deviation from the statistical value of unity is largely due to valence-Rydberg mixing.

Thus, albeit the theory predicts an enhancement of $(I_L/I_H)_{direct}$ compared to the statistical ratio it is not in quantitative agreement with the measured intensity ratio. To explain the difference we consider the CVR process, which in this case would be autoionization of resonantly excited neutral N_C-excited states to an ionized N_T core hole state. Such nearest-neighbor-atom core hole transfer has only recently been observed in isolated molecules [18], and it is well known that the associated rate is small. In this specific case, however, the outgoing electron has much less energy than in the cases so far considered. Here the overlap between the continuum wave function and the orbital from where the electron comes cannot be neglected, as for core hole transfer processes with fast outgoing electrons [19]. Therefore, Γ_{CVR} may be substantially larger than the rate for the core hole transfer processes considered so far [20]. Since an intermediate-state Rydberg orbital probably would not give sufficient magnitude of f_H^R and Γ_{CVR}, the CVR interpretation

also must rely on substantial σ^* character of the neutral N_C-excited states in the vicinity of the N_T threshold [20]. In the absorption spectrum some intensity can, indeed, be assigned to N_C $1s$-σ^*-type transitions at the threshold of terminal nitrogen [21]. Therefore, we cannot exclude that this CVR process influences the XETECO spectrum of N_2O.

At the low-energy flank of the main peaks all XETECO spectra show excess intensity compared to the model fit (Figs. 1–3). We attribute such structures to electrons emitted subsequent to the radiative decay: valence hole states with a highly excited Rydberg electron decay with the emission of a slow electron. Such processes give rise to structures below the ionization threshold and influence the line shape of the main threshold peaks. Presently, this sets the limit for the quantitative analysis of the XETECO spectrum. Theoretical developments are called for to describe the XETECO results. In a rigorous treatment the whole process should be regarded as an inelastic photon scattering event [22], rather than within the approximate multistep model we have used in this paper. Complications arising due to vibronic coupling are also beyond the simple discussions presented here.

In conclusion, XETECO spectroscopy has been developed to a level where new details regarding core level ionization dynamics can be learned. The XETECO intensities in small molecules with close-lying core levels have been discussed in terms of direct threshold ionization cross sections and contributions from fast CVR autoionization processes.

[1] M. Schmidbauer *et al.*, J. Chem. Phys. **94**, 5299 (1991).

[2] U. Hergenhahn *et al.*, J. Phys. Chem. A **105**, 5704 (2001).

[3] L. J. Medhurst *et al.*, Chem. Phys. Lett. **193**, 493 (1992).

[4] T. Baer and P.-M. Guyon, in *High-resolution Laser Photoionization and Photoelectron Studies*, edited by I. Powis, T. Baer, and C.-Y. Ng (Wiley, Chichester, England, 1995).

[5] J.-E. Rubensson *et al.*, Phys. Rev. Lett. **76**, 3919 (1996).

[6] H. Lefebvre-Brion and R. W. Field, *Perturbations in the Spectra of Diatomic Molecules* (Academic Press, London, 1986), Chap. 7.

[7] K. C. Prince *et al.*, J. Synchrotron Radiat. **5**, 565 (1998).

[8] S. Cvejanovic and F. H. Read, J. Phys. B **7**, 1180 (1974).

[9] Y. Shimizu *et al.*, J. Electron Spectrosc. Relat. Phenom. **114–116**, 63 (2001).

[10] P. Glans *et al.*, J. Electron Spectrosc. Relat. Phenom. **82**, 193 (1996).

[11] N. Kosugi, Chem. Phys. **289**, 117 (2003).

[12] S. Sorensen *et al.* (unpublished).

[13] P. Glans *et al.*, J. Phys. B **26**, 663 (1993).

[14] P. Glans *et al.*, Phys. Rev. Lett. **76**, 2448 (1996).

[15] L. Pettersson *et al.*, J. Phys. B **17**, L279 (1984).

[16] K. Kaufmann *et al.*, J. Phys. B **22**, 2223 (1989).

[17] U. Fano and J. W. Cooper, Rev. Mod. Phys. **40**, 441 (1968).

[18] R. Guillemin *et al.*, Phys. Rev. Lett. **92**, 223002–2 (2004).

[19] R. Santra and L. S. Cederbaum, Phys. Rev. Lett. **90**, 153401 (2003).

[20] L. S. Cederbaum (private communication).

[21] J. Adachi *et al.*, J. Chem. Phys. **102**, 7369 (1995).

[22] T. Åberg and B. Crasemann, in *Resonant Anomalous Scattering*, edited by G. Materlik, C. J. Sparks, and K. Fischer (Elsevier, New York, 1994), p. 431.